

# Ventricular Activity Signal Removal in Atrial Electrograms of Atrial Fibrillation

Bahareh Abdi<sup>1</sup>, Richard C. Hendriks<sup>1</sup>, Alle-Jan van der Veen<sup>1</sup> and Natasja M. S. de Groot<sup>2</sup>

<sup>1</sup>*Circuits and Systems (CAS) Group, Delft University of Technology, Delft, The Netherlands*

<sup>2</sup>*Department of Cardiology, Erasmus University Medical Center, Rotterdam, The Netherlands*

**Keywords:** Atrial and Ventricular Source Separation, Low-rank and Sparse Matrix Decomposition, Atrial Fibrillation, Atrial Electrogram.

**Abstract:** Diagnosis and treatment of atrial fibrillation can benefit from various signal processing approaches employed on atrial electrograms. However, the performance and interpretation of these approaches get highly degraded by far-field ventricular activities (VAs) that distort the morphology of the pure atrial activities (AAs). In this study, we aim to remove VAs from the recorded unipolar electrogram while preserving the AA components. To do so, we have developed a framework which first removes the VA-containing segments and interpolates the remaining samples. This will also partly remove the atrial components that overlap with VA signals, e.g., during atrial fibrillation. To reconstruct the AA components, we estimate them from the removed VA-containing segments based on a low-rank and sparse matrix decomposition and add them back to the electrograms. The presented framework is of rather low complexity, preserves AA components, and requires only a single EGM recording. Instrumental comparison to template matching and subtraction and independent component analysis shows that the proposed approach leads to smoother results with better similarity to the true atrial signal.

## 1 INTRODUCTION

Atrial fibrillation (AF) is one of the most common age related cardiac arrhythmia whose persistence and progression is rooted in impaired electrical conduction known as electropathology. Atrial electrograms (EGMs), i.e. a record of changes in the electrical potential of the (many) cells in the neighborhood of an electrode that is positioned on the heart surface, play an important role in the analysis of AF and examining the level of electropathology in human tissue (Yaksh et al., 2015). However, these electrograms suffer from far-field ventricular activities (VAs) caused by ventricular depolarizations. Although during sinus rhythm (SR), atrial activity (AA) and VA are separated in time, they might overlap during AF. These strong VAs distort the morphology of the pure AAs, complicate their further analysis and affect their final interpretations. Therefore, a required step before any further processing of the recorded electrograms is to estimate the pure atrial activities by removing the VAs.

Reita et al. in (Reita and Hornero, 2007) categorizes the developed algorithms for VA removal into three groups. The first group of algorithms is based

on template matching and subtraction (TMS) (Shkurovich et al., 1998). A second group is based on adaptive filtering using a VA reference (Petruțiu et al., 2006), which is obtained using a reference ECG lead. The third group of VA removal algorithms is based on blind source separation approaches that try to separate the components based on the assumption that VA and AA are uncorrelated, orthogonal, or statistically independent from beat to beat over time or over space in multichannel recordings. Independent component analysis (ICA) is one of the most widely used approaches from this group (Reita et al., 2004). None of above mentioned approaches results in a pure AA estimate. A perfect performance, however is hampered by the fact that these signals share overlapping components in both time and frequency domain and are also partially correlated over time and space.

In this study we develop a new framework for removing VA which is based on a sparse and low rank matrix decomposition. Initially, VA-containing segments are detected, removed and replaced with subsequent spline interpolation. However the performance of this approach is limited during AF, as VAs might overlap with the depolarization phase of AAs. In our approach, we propose to reconstruct AAs in the remo-

ved segments and adding them back to the interpolated signal. Finally, using simulations, we compare the performance of the proposed algorithm with two other approaches, TMS and ICA.

The remainder of this paper is as follows. In Section 2 we formulate the ventricular and atrial activity separation problem and present our proposed framework for solving the problem. In Section 3 we present the results and compare them with two other methods. Finally, in Section 4, conclusions are drawn.

## 2 METHOD

### 2.1 Electrogram Model

We consider a sampled unipolar atrial electrogram  $\mathbf{m} \in \mathbb{R}^{N \times 1}$  with  $N$  the number of time samples. We assume that  $\mathbf{m}$  is the summation of AAs and VAs, modeled as

$$\mathbf{m} = \mathbf{a} + \mathbf{v}, \quad (1)$$

where vectors  $\mathbf{a}$ , and  $\mathbf{v}$  contain the AA and VA samples produced by atrial and ventricular sources respectively. From the physiological point of view, the AA is composed of two phases, the depolarization phase and the repolarization phase. The depolarization phase is of most interest and consists of a predominantly positive spike followed by a sharp negative deflection. It mostly contains high frequency AA components and shows a sparse representation in time. The repolarization phase on the other hand, changes very smoothly in time and contains very low frequency components. These repolarization activities are often viewed as baseline wandering and may even fade out in some recordings. Depending on the homogeneity of the depolarization wavefront and the speed of the electrical propagation in the tissue, the morphology of these two components may vary from activity to activity even during SR and they cannot be simply considered as a shifted version of each other, especially during AF.

### 2.2 Data Matrix Formation

To overcome the unnecessary introduction of artifacts, we use the concept of minimal processing and process only VA-containing segments. In this study, we used a simultaneously recorded ECG as reference signal to specify the VA-containing segments in the electrogram which coincide with the QRS complexes in ECG. Since the QRS complex or the R peak is easily detectable, any simple detection algorithm could be used. A rectangular window centered at each detected R peak with a fixed width  $W$  is used to mark

the onset and offset of the VA and to denote the VA-containing segments that might also contain AA during AF.

The baseline wandering of the electrogram is mainly caused by the repolarization phase of AA. To remove the VA without affecting this component, we first remove the VA-containing segments and then replace them by spline interpolation applied on the remaining data samples. This can to some extent replace the removed baseline in the VA segment and is one of the most basic and efficient approaches for VA cancellation during SR (Ahmad et al., 2011). The interpolated data is denoted by  $\mathbf{m}'$  and has the same length as the recorded electrogram  $\mathbf{m}$ . During SR and in some cases during AF, the VA does not overlap with the depolarization phase of AA, and leaves this component unaffected. Removal and interpolation cancels the VAs thus sufficiently and no further processing would be necessary, cf. the input signal  $\mathbf{m}$  and interpolated signal  $\mathbf{m}'$  in the first VA-containing segment of Figure 1. However, unlike during SR, it is likely that during AF the depolarization phase of the AA and the VA completely or partially overlap. In this case VA removal and interpolation also removes the overlapping depolarization phase of AA. Therefore, processing the removed component, i.e.,  $\mathbf{x} = \mathbf{m} - \mathbf{m}'$ , is required to extract the potentially removed atrial components and add them back to the interpolated data, cf. the  $\mathbf{m}$ ,  $\mathbf{m}'$  and the removed signal  $\mathbf{x}$  in the second and third VA-containing segments of Figure 1.

Before employing any further processing, we construct an appropriate data matrix  $\mathbf{X}$  of size  $W \times K$ , where each column of  $\mathbf{X} = [\mathbf{x}_1^T, \mathbf{x}_2^T, \dots, \mathbf{x}_K^T]^T$  is one VA-containing segment (of length  $W$ ) of  $\mathbf{x}$  stored in the vector  $\mathbf{x}_k$ ,  $k \in 1, 2, \dots, K$ , and where  $K$  is the total number of detected segments. The data matrix  $\mathbf{X}$  is modeled as the sum of two components (i) matrix  $\mathbf{V}$  containing the aligned ventricular activities and (ii) matrix  $\mathbf{A}$  containing the randomly occurring atrial activities that coincided with the VA-containing segment, i.e.

$$\mathbf{X} = \mathbf{A} + \mathbf{V}. \quad (2)$$

### 2.3 VA and AA Separation

We now formulate the problem of decomposing the data matrix  $\mathbf{X}$  into its two components,  $\mathbf{V}$  and  $\mathbf{A}$ . The problem can be considered as a highly under-determined blind source separation where the number of unknowns,  $\mathbf{A}$  and  $\mathbf{V}$ , is twice the number of given measurements,  $\mathbf{X}$ . However, prior knowledge of the two sources can be employed to derive useful approximate solutions: (i) The aligned VAs in  $\mathbf{V}$ ,

from beat-to-beat, have an almost similar morphology which indicates that  $\mathbf{V}$  is a low-rank matrix while the occurrence of AA and its morphology in these segments is random indicating that  $\mathbf{A}$  is not a low-rank matrix, (ii) When presented in frequency domain, the VAs are much sparser, and (iii) AAs are sharper and more spiky in time domain compared to VAs, matrix  $\mathbf{A}$  can therefore be constrained to be sparse. Exploiting these three properties, we formulate the separation problem as

$$\begin{aligned} \min_{\{\mathbf{A}, \mathbf{V}\}} \text{rank}(\mathbf{V}) + \beta \|\Psi^T \mathbf{V}\|_1 + \alpha \|\mathbf{A}\|_1 \\ \text{s. t. } \mathbf{X} = \mathbf{A} + \mathbf{V}, \end{aligned} \quad (3)$$

where  $\text{rank}(\cdot)$  is the rank operator,  $\|\mathbf{A}\|_1 = \sum_{ij} |A_{ij}|$  is the  $l_1$ -norm of  $\mathbf{A}$ ,  $\Psi^T$  performs the two-dimensional cosine transform (DCT), and  $\alpha$  and  $\beta$  are the penalization parameters.

Since the rank function is non-differentiable and non-convex, it is in most studies approximated with the nuclear norm,  $\|\mathbf{V}\|_* = \sum_{i=1}^K \sigma_i(\mathbf{V})$ , that is the summation of all sorted (from largest to smallest) singular values  $\sigma_i$  of matrix  $\mathbf{V}$ . However, minimizing the truncated nuclear norm (TNN)  $\|\mathbf{V}\|_r = \sum_{k=r+1}^K \sigma_k(\mathbf{V})$ , that is the summation of the  $K - r$  smallest singular values, performs better in minimizing the rank function than minimizing the nuclear norm (Hu et al., 2013). The TNN, on the other hand, is non-convex and it cannot be minimized directly. To overcome this issue, the TNN is initially approximated by its convex surrogate (Hu et al., 2013)

$$\begin{aligned} \|\mathbf{V}\|_r &= \sum_{i=r+1}^K \sigma_i(\mathbf{V}) = \|\mathbf{V}\|_* - \sum_{i=1}^r \sigma_i(\mathbf{V}) \\ &= \|\mathbf{V}\|_* - \max_{\mathbf{U}_r, \mathbf{U}_r^T = \mathbf{I}, \mathbf{H}_r, \mathbf{H}_r^T = \mathbf{I}} \text{Tr}(\mathbf{U}_r \mathbf{V} \mathbf{H}_r^T), \end{aligned} \quad (4)$$

where  $\text{Tr}(\cdot)$  indicates the trace of a matrix, and  $\mathbf{U}_r$  and  $\mathbf{H}_r$  are matrices containing the first  $r$  columns of the left and right singular vectors of  $\mathbf{V}$  respectively, where  $\mathbf{V} = \mathbf{U} \text{diag}(\boldsymbol{\sigma}) \mathbf{H}^T$  is the singular value decomposition (SVD) of  $\mathbf{V}$ . Using Equation (4), the new optimization problem for separation of VA and AA can be written as

$$\begin{aligned} \min_{\{\mathbf{A}, \mathbf{V}\}} \{ \|\mathbf{V}\|_* - \max_{\mathbf{U}_r, \mathbf{U}_r^T = \mathbf{I}, \mathbf{H}_r, \mathbf{H}_r^T = \mathbf{I}} \text{Tr}(\mathbf{U}_r \mathbf{V} \mathbf{H}_r^T) \\ + \beta \|\Psi^T \mathbf{V}\|_1 + \alpha \|\mathbf{A}\|_1 \} \\ \text{s. t. } \mathbf{X} = \mathbf{A} + \mathbf{V}. \end{aligned} \quad (5)$$

Generally, the lower  $K$  (i.e., the number of VA-containing segments in  $\mathbf{M}$ ), the less accurate the SVD will be. This might lead to AA components erroneously ending up in the low-rank matrix  $\mathbf{V}$ . Constraining  $\mathbf{V}$  to be sparse in the frequency domain using the

$l_1$  regularization on  $\Psi^T \mathbf{V}$  overcomes that AA components, that are constrained to be sparse in time domain, end up in the  $\mathbf{V}$  matrix. Notice that we did not extensively search for efficient dictionaries for  $\Psi$ . However, we found that the application of the DCT was computationally of rather low complexity, while leading to good performance.

A variety of numerical approaches can be used to solve the optimization problem in Equation (5), among which we opt for the alternating direction method of multipliers (ADMM) (Boyd et al., 2011). This algorithm solves a convex optimization problem by breaking it into smaller pieces which are simpler to implement. Furthermore, ADMM has a fast convergence rate to a reasonable precision in practice. To solve Equation (5), we follow the same approach and algorithmic steps introduced in (Xue et al., 2018). The estimated AAs in  $\mathbf{A}$  are added back to the corresponding samples in the interpolated electrogram  $\mathbf{m}'$  using a rectangular window. This results in the final estimated atrial activity  $\hat{\mathbf{a}}$ . The ventricular activities in  $\mathbf{V}$  are also added to their corresponding samples in a zero signal of same length as  $\mathbf{m}$  using a rectangular window.

### 3 RESULTS

The proposed framework, from here on referred to as low-rank and sparse matrix decomposition (LRSD) method, is tested on clinically recorded epicardial unipolar electrograms. The electrograms consist of 10 s of induced AF signals recorded at similar locations on the right atrium of multiple patients, filtered (bandwidth 0.5 to 400 Hz) and sampled (1 kHz). More details on the electrode specifications can be found in (Yaksh et al., 2015). To provide a clear understanding of the steps of the algorithm and enable visual inspection of the results, we initially employ it on the clinically recorded data and demonstrate the output of each step. However, in Section 3.2 a more detailed evaluation will be performed on synthetic data. The results are evaluated using instrumental measures and will also be compared with TMS and ICA approaches.

#### 3.1 Experiments on Clinical Data

Figure 1 visualizes a fragment of each stage of the proposed framework, employed on 10 s of clinically recorded electrogram during induced AF. The electrogram is normalized such that the average ventricular activity has a maximum amplitude of -1. The 10 seconds contain  $K = 16$  VA-containing segments, each

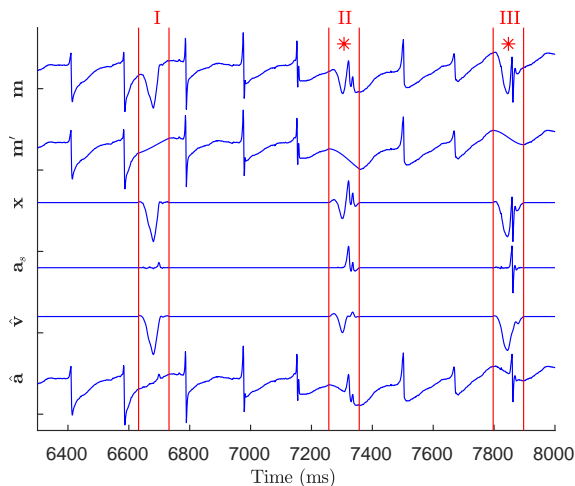


Figure 1: The input electrogram  $\mathbf{m}$  and output signals at each stage of the algorithm with  $\hat{\mathbf{v}}$  and  $\hat{\mathbf{a}}$  as the final extracted VA and AA output. The onset and offset of VA-containing segments are denoted by red vertical lines. The segments where AA and VA overlap are also denoted by \*.

windowed with a rectangular window with a fixed length of  $W = 100$  samples (100 ms). Since the focus of this study is on introducing the algorithm itself and not on optimal tuning of its parameters, we used values that yielded visually good source separation, that are,  $\alpha = 0.5$ ,  $\beta = 0.8$ , and  $r = 3$ .

The input signal is shown as  $\mathbf{m}$  in Figure 1. The VA-containing segments are initially removed and interpolated and the result is shown as  $\mathbf{m}'$ . LRSD is employed on the data matrix  $\mathbf{X}$  containing the VA-containing segments of  $\mathbf{x} = \mathbf{m} - \mathbf{m}'$ . The separated atrial and ventricular activities resulting from the LRSD are plotted as  $\mathbf{a}_s$  and  $\hat{\mathbf{v}}$  respectively.  $\hat{\mathbf{a}} = \mathbf{a}_s + \mathbf{m}'$  demonstrates the final atrial activity estimated from the input signal  $\mathbf{m}$ . For an easier visual inspection, we show for both  $\hat{\mathbf{a}}$  and  $\hat{\mathbf{v}}$  in Figure 2 a zoomed version of 3 VA-containing segments from the example in Figure 1.

To compare the performance of the algorithm with two other approaches we select the TMS (Shkurovich et al., 1998) and ICA (Rieta et al., 2004) approaches. TMS, similar to the LRSD, only requires one electrogram as well as the ECG signal for detection of VA-containing segments and is computationally of low complexity. However, to separate the two sources, ICA requires the whole ECG signal. Moreover, taking care of the permutation and scaling in the result of ICA is complicated and can affect its performance. Figure 3 demonstrates four clinically recorded electrograms  $\mathbf{m}$  from four different patients as well as the three estimated atrial components for each patient. As we can see, LRSD visually provides the best and smoothest output. The smoothness of the atrial com-

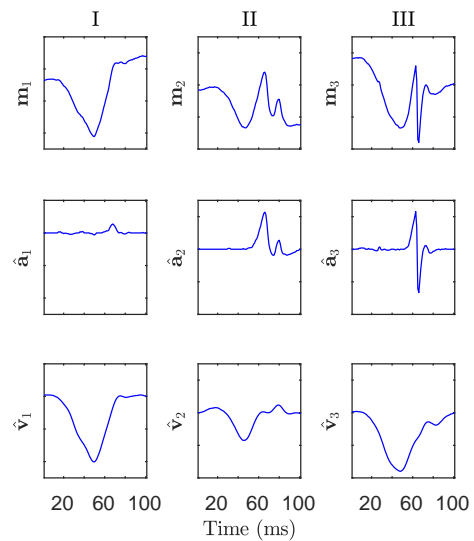


Figure 2: Zoomed version of the three specified VA-containing segments in Figure 1 as well as  $\hat{\mathbf{v}}$  and  $\hat{\mathbf{a}}$  as the final extracted atrial and ventricular activity.

ponent is of high importance for further processing of the data, since any added distortion might be misinterpreted as fractionated AAs.

### 3.2 Performance Evaluation

Evaluating the performance of the proposed method using instrumental measures, requires the pure AA and VA, which are not available from clinically recorded data. On the other hand, due to the big range of variations in AAs and VAs morphology during AF, generating realistic data for a fair performance evaluation is difficult. To avoid these complications and test the framework on realistic data, we generated the synthesized data in two steps. First we select a sample VA-containing segment from the electrogram and we make sure it does not coincide with AA. We then extract the VA in this segment using spline interpolation and subtraction. Since VA does not overlap with AA, this provides us with well separated AA and VA components. The separated VA, referred to as pure VA, is then added to another location on the same EGM where it overlaps with pure AA and not with another VA. The pure VA is also shifted in small steps (10 ms) to create different degrees of overlap with the AA. The same steps are also performed on the ECG signal. Finally, TMS, ICA, and LRSD are employed on the synthesized data.

To evaluate the performance of the introduced approaches in separating the AA and VA components, we use four different instrumental measures. The first instrumental measure we use is the normalized cross-correlation coefficient between the pure AA  $\mathbf{a}$  and the

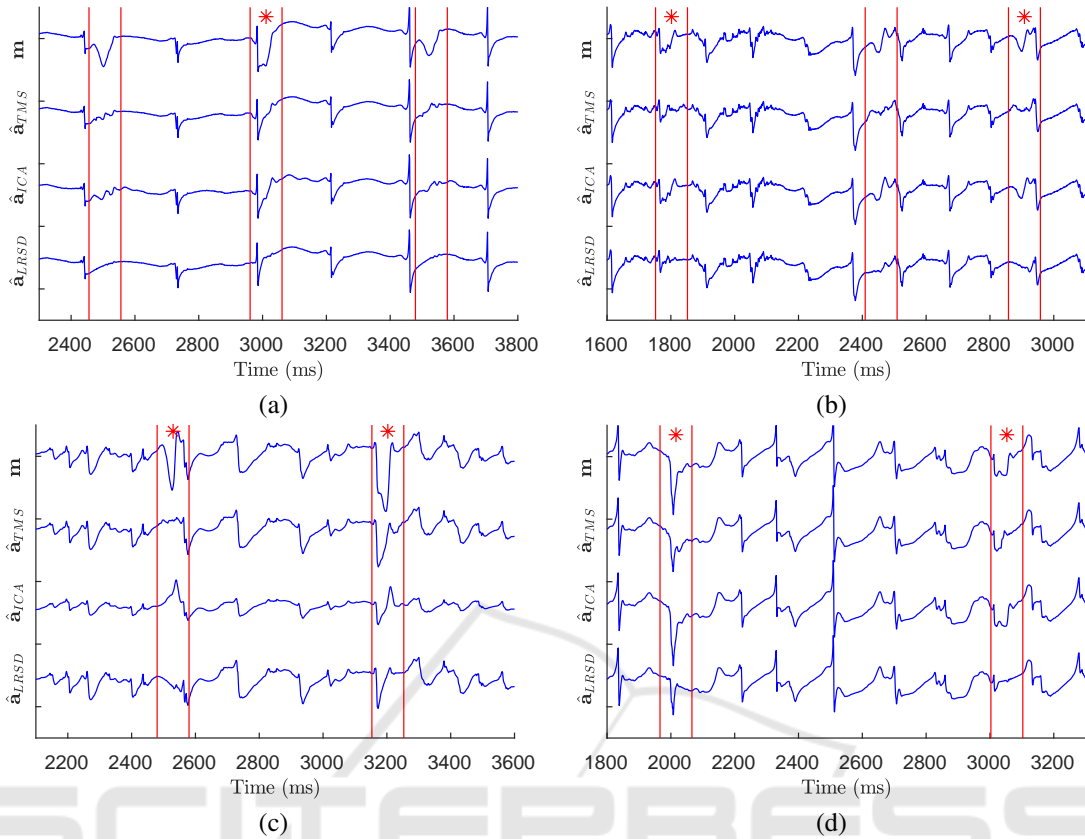


Figure 3: The signals from before are respectively the clinically recorded electrogram  $\mathbf{m}$  from four different patients (a) to (d), and the separated atrial activity after employing TMS, ICA and the LRSD. The vertical lines indicate the onset and offset of VA-containing segments. Overlapping AA and VA are indicated by \*.

extracted AA  $\hat{\mathbf{a}}$ , referred to as the similarity metric, that is

$$Si = \frac{\text{cov}(\mathbf{a}, \hat{\mathbf{a}})}{\text{std}(\mathbf{a})\text{std}(\hat{\mathbf{a}})}, \quad (6)$$

where  $\text{cov}(\cdot)$  is covariance and  $\text{std}(\cdot)$  is the standard deviation. The closer this variable is to 1, the more similar the signals are. The second instrumental measure is the mean square error (MSE) between  $\mathbf{a}$  and  $\hat{\mathbf{a}}$  denoted by  $MSE_a$ . The smaller this value is, the better the results. The third instrumental measure is the ventricular depolarization reduction (VDR) defined as (Rieta and Hornero, 2007)

$$\text{VDR} = \left| 1 - \frac{\max(|\hat{\mathbf{v}}|)}{\max(|\mathbf{v}|)} \right| \quad (7)$$

where  $\max(|\mathbf{v}|)$  is the maximum amplitude of ventricular activity that coincides with the R-peak in ECG and  $\max(|\hat{\mathbf{v}}|)$  is the maximum amplitude of extracted ventricular activity. The smaller the VDR is, the better the ventricular reduction. We also introduce a new instrumental measure that measures smoothness, abbreviated as  $Sm$ . It is calculated as the standard deviation of the first time derivative of the difference

Table 1: Summary of instrumental measures.

	$MSE_v$		Si	$MSE_a$	VDR	Sm
P1	0.005	TMS	<b>0.96</b>	<b>0.005</b>	<b>0.19</b>	<b>0.01</b>
		ICA	0.29	0.124	0.59	0.03
		LRSD	0.75	0.031	0.26	0.02
P2	0.008	TMS	0.89	0.008	0.13	0.01
		ICA	0.80	0.058	1.53	0.02
		LRSD	<b>0.97</b>	<b>0.007</b>	<b>0.06</b>	<b>0.01</b>
P3	0.021	TMS	0.82	0.02	0.25	0.01
		ICA	0.53	2.250	2.64	0.09
		LRSD	<b>0.86</b>	<b>0.01</b>	<b>0.04</b>	<b>0.01</b>
P4	0.071	TMS	0.71	0.07	0.32	0.04
		ICA	0.36	0.958	2.64	0.09
		LRSD	<b>0.84</b>	<b>0.038</b>	<b>0.15</b>	<b>0.03</b>
P5	0.148	TMS	0.68	0.148	0.28	0.07
		ICA	0.25	2.820	2.52	0.19
		LRSD	<b>0.79</b>	<b>0.038</b>	<b>0.15</b>	<b>0.03</b>

between  $\mathbf{a}$  and  $\hat{\mathbf{a}}$ , which is

$$Sm = \text{std} \left( \frac{d(\mathbf{a} - \hat{\mathbf{a}})}{dt} \right). \quad (8)$$

The smaller this value is, the less fractionated the results are.

Table 1 shows the results of the instrumental me-

asures evaluated on synthesized data of five different patients, where the VAs and AAs are separated using the three introduced approaches TMS, ICA and the LRSD. The patients are sorted based on the regularity in their VA-containing segments, where the mean square error between the average of all segments and the pure VA denoted by  $MSE_v$ , is used as the indicator of the regularity. For all patients, the added pure VA overlaps with several randomly selected AAs, with different levels of overlap, except for patient 2 where we purposely chose samples with no overlap with AA. The performance of ICA in our simulations is relatively bad. This might be partly due to (i) the low quality of the ECG signal we had access to in this experiment and (ii) the errors in handling the permutation and scaling issues in ICA.

As can be seen, the results with respect to similarity and MSE are quite comparable for all patients, however as the regularity in VA-containing segments decreases, the LRSD outperforms the other two approaches in almost all measures. Only for the first patient with very regular segments, TMS performs better than the proposed LRSD. As previously mentioned, the smoothness is of high importance since the added distortions might be misinterpreted as fractionated electrograms. However our simulations on synthesized data show that if the AA is already fractionated, the added distortions after employing TMS and ICA completely change the morphology of pure AA, while the LRSD preserves the pure AA morphology, resulting in better performances.

## 4 CONCLUSION

In this study we proposed a new framework for removal of VA from atrial electrograms, which is based on interpolation and subtraction followed by low-rank and sparse matrix decomposition. The proposed framework is of low complexity, does not require high resolution multi-channel recordings, or a calibration step for each individual patient. The approach outperforms the reference methods TMS and ICA with respect to instrumental measures. In particular in cases where the ventricular activities are less regular. It provides smooth AA estimates, which is of high importance for signal processing applications that are based on the fractionation evaluation in atrial activities.

## REFERENCES

- Ahmad, A., Salinet, J., Brown, P., Tuan, J. H., Stafford, P., Ng, G. A., and Schindwein, F. S. (2011). Qrs subtraction for atrial electrograms: flat, linear and spline interpolations. *Medical & biological engineering & computing*, 49(11):1321–1328.
- Boyd, S., Parikh, N., Chu, E., Peleato, B., Eckstein, J., et al. (2011). Distributed optimization and statistical learning via the alternating direction method of multipliers. *Foundations and Trends® in Machine Learning*, 3(1):1–122.
- Hu, Y., Zhang, D., Ye, J., Li, X., and He, X. (2013). Fast and accurate matrix completion via truncated nuclear norm regularization. *IEEE transactions on pattern analysis and machine intelligence*, 35(9):2117–2130.
- Petrutiu, S., Ng, J., Nijm, G. M., Al-Angari, H., Swiryn, S., and Sahakian, A. V. (2006). Atrial fibrillation and waveform characterization. *IEEE engineering in medicine and biology magazine*, 25(6):24–30.
- Rieta, J. J., Castells, F., Sánchez, C., Zarzoso, V., and Millet, J. (2004). Atrial activity extraction for atrial fibrillation analysis using blind source separation. *IEEE Transactions on Biomedical Engineering*, 51(7):1176–1186.
- Rieta, J. J. and Hornero, F. (2007). Comparative study of methods for ventricular activity cancellation in atrial electrograms of atrial fibrillation. *Physiological measurement*, 28(8):925.
- Shkurovich, S., Sahakian, A. V., and Swiryn, S. (1998). Detection of atrial activity from high-voltage leads of implantable ventricular defibrillators using a cancellation technique. *IEEE Transactions on Biomedical Engineering*, 45(2):229–234.
- Xue, Z., Dong, J., Zhao, Y., Liu, C., and Chellali, R. (2018). Low-rank and sparse matrix decomposition via the truncated nuclear norm and a sparse regularizer. *The Visual Computer*, pages 1–18.
- Yaksh, A., van der Does, L. J., Kik, C., Knops, P., Oei, F. B., van de Woestijne, P. C., Bekkers, J. A., Bogers, A. J., Allessie, M. A., and de Groot, N. M. (2015). A novel intra-operative, high-resolution atrial mapping approach. *Journal of Interventional Cardiac Electrophysiology*, 44(3):221–225.